

Pressure-induced depolarization and resonance in Raman scattering of single-crystalline boron carbide

著者	Guo Junjie, Zhang Ling, Fujita Takeshi, Goto Takashi, Chen Mingwei
journal or publication title	Physical Review. B
volume	81
number	6
page range	060102(R)
year	2010
URL	http://hdl.handle.net/10097/53640

doi: 10.1103/PhysRevB.81.060102

Pressure-induced depolarization and resonance in Raman scattering of single-crystalline boron carbide

Junjie Guo,¹ Ling Zhang,¹ Takeshi Fujita,¹ Takashi Goto,² and Mingwei Chen^{1,*}
¹WPI Advanced Institute for Materials Research, Tohoku University, Sendai 980-8577, Japan
²Institute for Materials Research, Tohoku University, Sendai 980-8577, Japan

(Received 6 December 2009; published 24 February 2010)

We report polarized and resonant Raman scattering of single-crystal boron carbide (B_4C) at high pressures. Significant intensity enhancements of 270 and 1086 cm^{-1} Raman bands of B_4C have been observed at quasi-hydrostatic pressures higher than ~ 20 GPa. The pressure-induced intensity change of the 1086 cm^{-1} band is mainly due to the resonance between excitation energy and electronic transition, whereas the intensity change of 270 cm^{-1} band is caused by the depolarization effect. Importantly, the first-order phase transition has not been found at high quasi-hydrostatic pressures and all the Raman intensity changes along with the corresponding high-pressure lattice distortion can be recovered during unloading.

DOI: [10.1103/PhysRevB.81.060102](https://doi.org/10.1103/PhysRevB.81.060102)

PACS number(s): 81.05.Je, 78.30.-j, 61.50.Ks, 07.35.+k

Low-density and ultrahard boron carbide (B_4C) possesses outstanding ballistic properties and has been widely used as an armor ceramic for protection against high-pressure impact.¹⁻³ Extensive investigations on microstructure and properties of B_4C have been conducted and, in particular, mechanical performances at high pressures and high loading rates have been the subject of much intense work over the last 30 years.^{2,4} B_4C has a complex atomic configuration, i.e., 12 atom icosahedra at the rhombohedral polar sites linked with each other through a linear three-atom chain parallel to the hexagonal C axis (see the inset in Fig. 1).^{5,6} Each atom at the two ends of the chain bonds to three boron atoms in the icosahedra. Accordingly, six equatorial sites (forming bonds with the linear chain) and six polar sites (forming bonds with the neighboring icosahedra) coexist in the 12 atom icosahedra. This intricate structure along with much open internal space in the less-symmetric unit cell has led to the supposition of possible equilibrium phase transitions at high hydrostatic pressures. Although recent studies have demonstrated localized amorphization in B_4C loaded by non-hydrostatic pressures,⁶⁻⁹ the equilibrium high-pressure phase transitions of B_4C remain undecided. High-pressure Raman studies have found unusual intensity changes of B_4C Raman bands at a pressure of ~ 20 GPa,^{9,10} which is coincident with the observation of the dramatic loss of B_4C shear strength at an impact pressure of ~ 20 GPa.^{2,4,6} The concurrence has brought about the suggestion of a rhombohedron to wurtzite phase transition at high pressures.^{10,11} However, this interpretation on the high-pressure Raman intensity changes does not reconcile with other experiments, such as x-ray diffraction and neutron scattering, in which this first-order phase transition has not been detected with the pressures up to 50 GPa.^{12,13} Besides phase transitions, it is known that pressure-induced lattice shrinkage and distortion can also give rise to the intensity changes of Raman bands because of the variations in symmetry selection rules and types of lattice vibrations. In this study, we systematically investigate high-pressure Raman scattering of single-crystal B_4C and demonstrate that the unusual Raman intensity changes at ~ 20 GPa are mainly caused by depolarized and resonant Raman scattering, not the first-order phase transition.

A diamond-anvil cell (DAC) combined with micro-Raman spectroscopy was employed to investigate the high-pressure Raman scattering of single-crystal B_4C with a selected orientation of (223). A mixture of methanol-ethanol (4:1) was used as the pressure transmitting medium and the R1-line emission of a tiny ruby chip was used for pressure calibration. Raman spectra were *in situ* acquired under pressures using a Renishaw micro-Raman spectrometer equipped with a charge-coupled device detector and a microscope for focusing the incident laser beam to a ~ 2 μm spot size. Both 514 nm (Ar ion laser) and 633 nm (He-Ne laser) excitation lines were used as excitation sources. The spectra have been collected at a lower laser power in order to avoid local heating effects. Polarization analyzer is placed before the entrance of slit to allow the detection of the scattered light either parallel (\parallel) or perpendicular (\perp) to the excitation laser. The ratio of the peak intensity (I) of the perpendicular and parallel components, known as the depolarization ratio (ρ), is obtained by $\rho = I_{\perp} / I_{\parallel}$. Since the measured depolarization effect is always interfered by diamond window of the pressure cell, ρ of B_4C is corrected by the depolarization

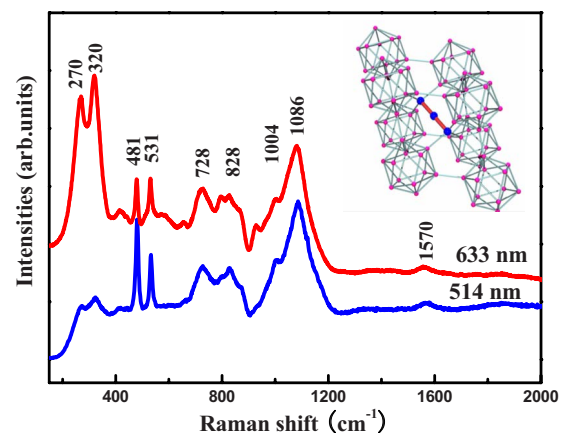


FIG. 1. (Color online) Raman spectra from (223) B_4C single crystal with 514 nm (Ar ion laser) and 633 nm (He-Ne laser) excitation sources, respectively. The inset shows the atomic configuration of B_4C .

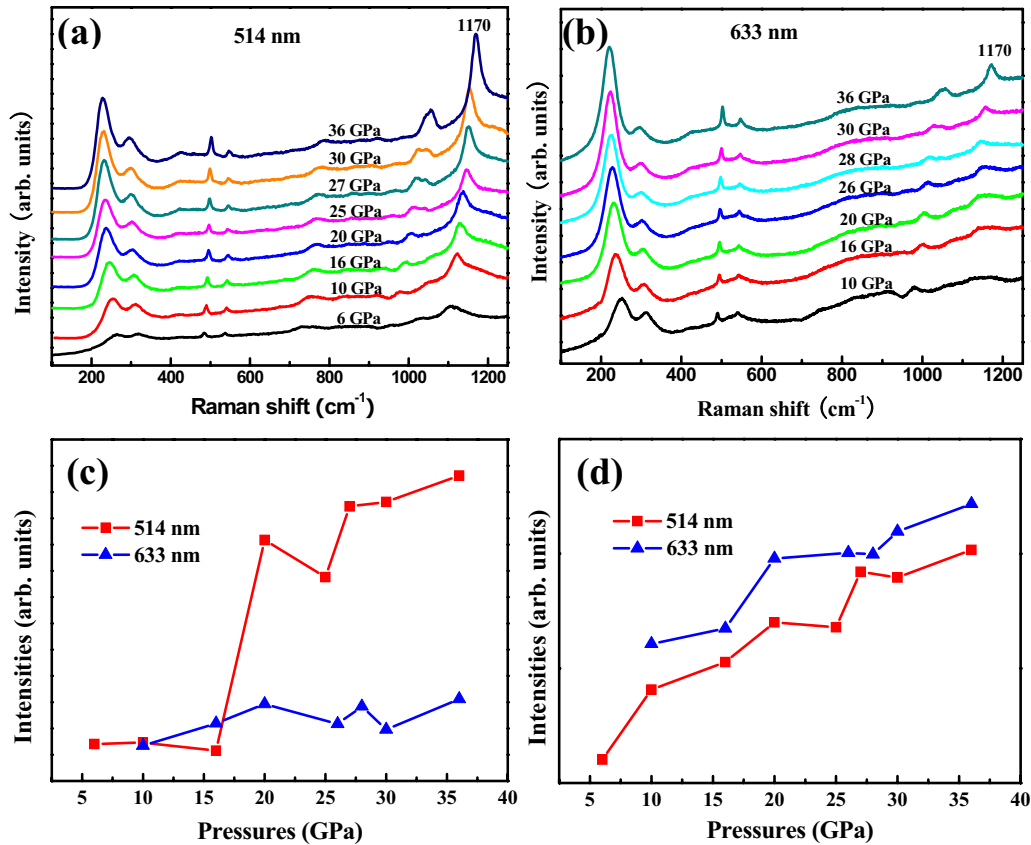


FIG. 2. (Color online) High-pressure Raman scattering of B_4C under the excitation of (a) 514 and (b) 633 nm laser lines. Pressure dependence of the intensities of Raman bands at (c) 1086 and (d) 270 cm^{-1} .

ratio of 1330 cm^{-1} peak of diamond. To 1330 cm^{-1} peak of stressed diamond, the focus plane of the laser beam is placed at the bottom of the diamond anvil where the window diamond is subjected to the highest stresses. The measured depolarization ratio change of the diamond window with pressures is of $\sim -0.05/GPa$, about 10–20 times smaller than those observed in B_4C . Figure 1 shows typical Raman spectra of the single-crystal (223) B_4C at ambient pressure with two excitation wavelengths of 514 and 633 nm, respectively. The spectra in the range of 150–2000 cm^{-1} with a series of characteristic Raman bands represent the complex atomic structure of B_4C , which are in good agreement with previous observations.^{7–9,14–16} In the low-frequency region, two bands at ~ 270 and ~ 320 cm^{-1} have been attributed to bond bending between the three-atomic chains and icosahedra due to chain rotating and icosahedra wagging.¹⁴ Apparently, the two bands are sensitive to the excitation lasers and have higher intensity at 633 nm excitation compared with the 514 nm laser. The sharp band at 481 cm^{-1} is associated with the stretching of three-atom chains and the 531 cm^{-1} mode represents the rigid rotation of icosahedra.^{14,17} In the high-frequency region, the multiple Raman bands ranging from 700 to 900 cm^{-1} have been assigned to the intraicosahedral or intericosahedral B-B bonds. The peaks at 900–1000 cm^{-1} are related to the modes of chain stretching and rotating, and the 1086 cm^{-1} peak corresponds to the breathing modes of the icosahedra.^{14,17} Apart from the vibration modes of B_4C , a weak and broadband at 1570 cm^{-1} was observed in the Ra-

man spectra. This peak is attributed to the so-called G peak (graphite peak) due to the presence of small amount of free C on the surface of B_4C specimens.^{16,18}

Figures 2(a) and 2(b) show Raman spectra of B_4C with the applied pressures gradually increasing from the ambient up to ~ 36 GPa under the excitations of 514 and 633 nm lasers, respectively. In both cases the changes in the Raman peak shift and intensity can be readily observed. With the increase in pressures, the B_4C Raman bands at 270 and 320 cm^{-1} slightly shift to lower frequencies, implying soft phonons associated with B_4C lattice distortion at high pressures.¹⁹ In contrast, the modes in the region between 400 and 1200 cm^{-1} gradually shift to higher frequencies. The most noticeable changes are the sharpening and intensity increase of the 270 and 1086 cm^{-1} bands at the pressure above ~ 20 GPa, which has been attributed to the possible structural phase transition.^{10,11} However, the dramatic enhancement of the 1086 cm^{-1} band at ~ 20 GPa, which is observed with 514 nm excitation, is absent with 633 nm excitation wavelength as shown in Fig. 2(c). The dependence of intensity increment on the excitation wavelength and the absence of new Raman bands unambiguously demonstrate that the intensity change of the 1086 cm^{-1} band is not associated with any first-order phase transition. The 1086 cm^{-1} band has a symmetry assignment of A_{1g} and originates from icosahedral breathing modes. The relatively weakly bonded icosahedron cages are expected to undergo the most compression according to the distinct blueshift of this mode with

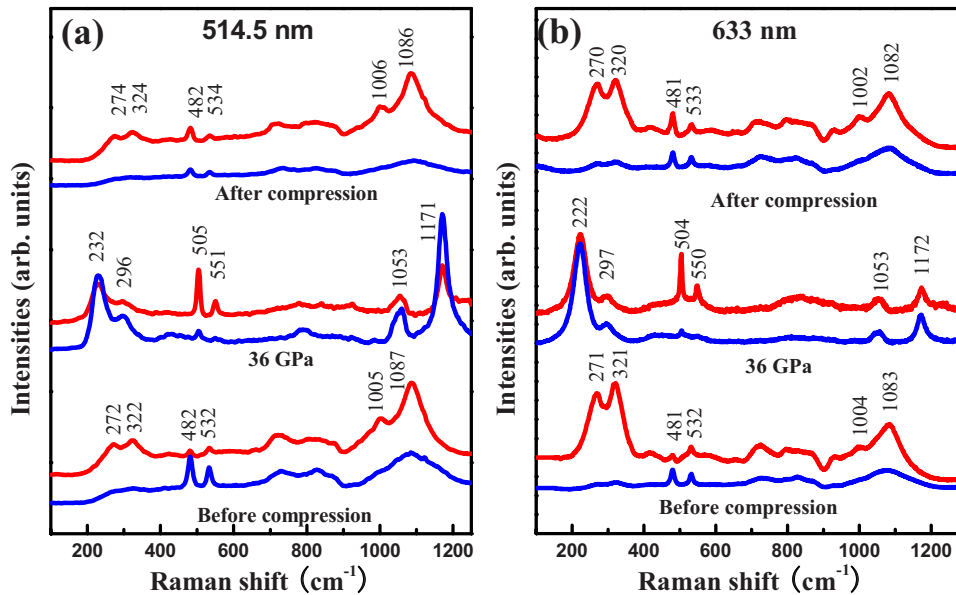


FIG. 3. (Color online) Parallel (I_{\parallel}) and perpendicular (I_{\perp}) components of the Raman spectra from pristine B_4C crystal, B_4C at 36 GPa, and recovered sample with the excitation of (a) 514 and (b) 613 nm lasers.

pressures.²⁰ In general, the energy of the exciting photon in linear Raman spectroscopy is much lower than the energy of the lowest electronic transitions in solids and molecules. If the latter energy is tuned to approach the energy of the exciting photons, the vibrational modes associated with the electronic transitions exhibit greatly enhanced Raman scattering intensity due to the resonance between electronic and vibrational excitations.²¹ For B_4C , the band gap and thereby electronic transition of icosahedra can be dramatically modified by high pressures²² and, as the pressures increase, the band gap between the excited and ground states is tuned for matching the energy of the exciting photons. The resonance enhancement can be achieved in advance by the 514 nm laser due to its higher excitation energy (2.41 eV) compared to 1.69 eV of the 633 nm laser.

We notice that the low-frequency peak at ~ 270 cm^{-1} shows strong pressure dependence for both excitation wavelengths, which is different from the 1086 cm^{-1} mode. To explore the underlying mechanisms, polarized Raman spectra were measured to characterize the high-pressure polarizability of lattice vibrations, which is sensitive to the lattice distortion. The parallel and perpendicular spectra of B_4C at ambient pressure and 36 GPa as well as the recovered samples are shown in Fig. 3. It is perceptible that the peak intensity of the ambient-pressure Raman spectra, particularly 270 and 320 cm^{-1} bands, shows strong dependence on the polarized orientations regardless of the excitation wavelengths, demonstrating that these two bands are highly polarized with low depolarization ratios. At the high pressure of 36 GPa, the relative intensity change of 270 and 320 cm^{-1} bands with polarized orientations becomes small, although the peak intensity ratio between 270 and 320 cm^{-1} bands increases with pressures. Since polarized Raman spectroscopy can provide information about the symmetry of the vibration, it can facilitate the observation of the pressure-induced lattice changes. The 270 and 320 cm^{-1} doublets in the lower frequency range are related to the chain-icosahedral linkages (A_{1g}) (Ref. 16) and are sensitive to the structural change at the end sites of the chains. Noticeably,

the next two narrow peaks (at 481 and 531 cm^{-1}) show the opposite changing tendency of polarizability with pressures in comparison with the 270 and 320 cm^{-1} bands. These two bands are associated with the stretching of three-atom chains and the rigid rotation of icosahedra, respectively. Eigenvectors associated with these two modes belong to the E_g irreducible representation. This phenomenon is consistent with the Raman selection rules that the relative intensity of the E_g modes varies inversely with that of A_{1g} modes between parallel and perpendicular polarizations.^{23,24} In addition to resonance excitation due to the variations with respect to pressures, 1086 cm^{-1} Raman band is also slightly polarized. It is worth noting that the bandwidth of 1086 cm^{-1} mode decreases noticeably under pressures. This is in contrast with the behavior of the other Raman bands which either show very little change in the bandwidth or become broader at higher pressures. More symmetrical icosahedra under pressures may explain the much narrower 1086 cm^{-1} band in compression. The similarity in the polarized Raman spectra between the pristine samples and the recovered B_4C crystals that are taken out from the DAC reveals that the lattice changes at high quasihydrostatic pressures are elastically reversible.

When Raman spectra are excited by plane-polarized radiation, the scattered radiation will be polarized to various degrees depending on the type of vibration responsible for the scattering. The intensity of resulting Raman bands will be stronger in certain spatial directions. In general, if the depolarization ratio ρ for a particular peak is less than 0.75, the peak arises from a totally symmetric vibrational mode. This peak or vibration is called a polarized band. If nonsymmetrical modes have a depolarization ratio larger than 0.75, they are called depolarized bands. The Raman bands at 270 and 320 cm^{-1} are A_{1g} -type totally symmetric modes for equatorial pentagons of three icosahedra and the corresponding atoms move approximately parallel to the plane of the equilateral triangle. The local lattice polarizability, which is responsible for the Raman intensity, strongly depends on the immediate surrounding of the active center and is attributed

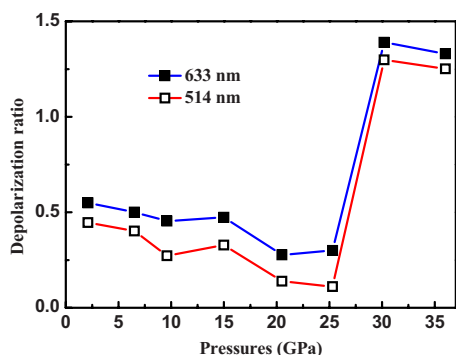


FIG. 4. (Color online) Pressure dependence of the depolarization ratios of the Raman band at 271 cm^{-1} .

to a total symmetrical vibration of pentagonal pyramids of icosahedra relative to the end atoms of the chain.²⁵ The depolarization ratio of the 270 cm^{-1} band at various pressures has been determined from the integrated Raman intensity obtained with perpendicular polarization (I_{\perp}) and parallel polarizations (I_{\parallel}). The depolarization ratio as a function of pressures has been plotted in Fig. 4. The variations of depolarization ratios reflect various polarization configurations and disposition of the vibration relative to the crystal axes. The ratio first decreases with the increase in pressure up to ~ 25 GPa and then dramatically increases with the continuous augment of loading pressures. The totally symmetric mode is first polarized with a depolarization ratio close to

zero at $\sim 20\text{--}25$ GPa and then the significant increase in depolarization ratios at higher pressures suggests that the symmetric vibration changes from isotropic to anisotropic. This can be attributed to the “wrong” geometry to a small violation of the selection rules coming from the changes in the local ordering at the linkages between icosahedra and chains, which should be the cause of the discontinuous intensity change of 270 cm^{-1} band at the pressure of ~ 20 GPa.^{8,9,26}

In summary, we systematically investigate the pressure dependence of the polarized and resonant Raman scattering of B_4C . The Raman band at 1086 cm^{-1} is resonantly enhanced due to the resonance between excitation energy and the electronic transitions varied with applied pressures. Depolarization effect is proved to be the main cause of the significant intensity enhancement of the Raman band at 270 cm^{-1} at high pressures. Importantly, the first-order phase transition suggested before has not been found in our study and all the Raman intensity changes along with corresponding high-pressure lattice distortion can be recovered after removing the quasihydrostatic stresses.

This work was supported by Global COE Program “Materials Integration (International Center of Education and Research), Tohoku University” and “World Premier International (WPI) Center Initiative for Atoms, Molecules and Materials,” MEXT, Japan.

*Author to whom correspondence should be addressed; mwchen@wpi-aimr.tohoku.ac.jp

¹F. Thevenot, *J. Eur. Ceram. Soc.* **6**, 205 (1990).

²D. P. Dandekar, Army Research Laboratory Report No. ARL-TR-2456, 2001 (unpublished).

³M. W. Chen, J. W. McCauley, J. C. LaSalvia, and K. J. Hemker, *J. Am. Ceram. Soc.* **88**, 1935 (2005).

⁴D. E. Grady, Sandia National Laboratories Report No. SAND 94-3266, 1995 (unpublished).

⁵R. Lazzari, N. Vast, J. M. Besson, S. Baroni, and A. Dal Corso, *Phys. Rev. Lett.* **83**, 3230 (1999).

⁶M. W. Chen, J. W. McCauley, and K. J. Hemker, *Science* **299**, 1563 (2003).

⁷V. Domnich, Y. Gogotsi, M. Trenary, and T. Tanaka, *Appl. Phys. Lett.* **81**, 3783 (2002).

⁸D. Ge, V. Domnich, T. Juliana, E. A. Stach, and Y. Gogotsi, *Acta Mater.* **52**, 3921 (2004).

⁹X. Q. Yan, Z. Tang, L. Zhang, J. J. Guo, C. Q. Jin, Y. Zhang, T. Goto, J. W. McCauley, and M. W. Chen, *Phys. Rev. Lett.* **102**, 075505 (2009).

¹⁰M. H. Manghnani, Y. Wang, F. Li, P. Zinin, and W. Rafaniello, *Science and Technology of High Pressure* (Universities Press, Hyderabad, India, 2000), pp. 945–948.

¹¹T. J. Holmquist and G. R. Johnson, *J. Appl. Phys.* **100**, 093525 (2006).

¹²M. Somayazulu, J. Akella, S. T. Weir, D. Hausermann, and G. Shen (unpublished).

¹³R. J. Nelmes, J. S. Loveday, R. M. Wilson, W. G. Marshall, J. M.

Besson, S. Klotz, G. Hamel, T. L. Aselage, and S. Hull, *Phys. Rev. Lett.* **74**, 2268 (1995).

¹⁴D. R. Tallant, T. L. Aselage, A. N. Campbell, and D. Emin, *Phys. Rev. B* **40**, 5649 (1989).

¹⁵T. L. Aselage, D. R. Tallant, and D. Emin, *Phys. Rev. B* **56**, 3122 (1997).

¹⁶X. Q. Yan, W. J. Li, T. Goto, and M. W. Chen, *Appl. Phys. Lett.* **88**, 131905 (2006).

¹⁷U. Kuhlmann and H. Werheit, *J. Alloys Compd.* **205**, 87 (1994).

¹⁸D. Ghosh, G. Subhash, T. S. Sudarshan, R. Radhakrishnan, and X. L. Gao, *J. Am. Ceram. Soc.* **90**, 1850 (2007).

¹⁹D. Machon, P. Bouvier, P. Tole'dano, and H. P. Weber, *J. Phys.: Condens. Matter* **18**, 3443 (2006).

²⁰A. M. Heyns, P. M. Harden, and L. C. Prinsloo, *J. Raman Spectrosc.* **31**, 837 (2000).

²¹Z. Z. Ho, R. C. Hanson, and S. H. Lin, *J. Phys. Chem.* **89**, 1014 (1985).

²²D. S. Jiang, Z. P. Wang, C. Abraham, K. Syassen, Y. H. Zhang, and K. Ploog, *J. Phys. Chem. Solids* **56**, 397 (1995).

²³V. Likodimos, T. Stergiopoulos, P. Falaras, J. Kunze, and P. Schmuki, *J. Phys. Chem. C* **112**, 12687 (2008).

²⁴N. Vast, S. Baroni, G. Zerah, J. M. Besson, A. Polian, M. Grimsditch, and J. C. Chervin, *Phys. Rev. Lett.* **78**, 693 (1997).

²⁵U. Kuhlmann and H. Werheit, *Phys. Status Solidi B* **175**, 85 (1993).

²⁶X. Blase, Philippe Gillet, A. San Miguel, and P. Mélinon, *Phys. Rev. Lett.* **92**, 215505 (2004).